

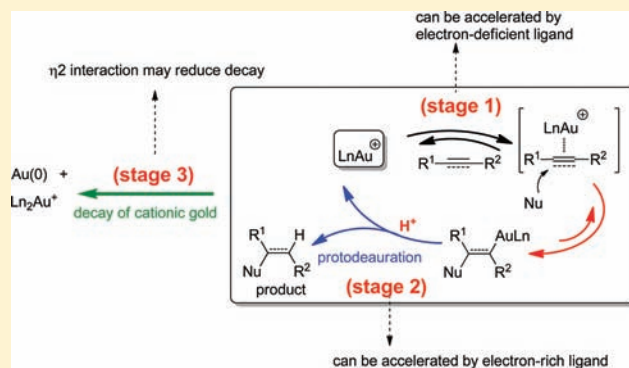
# Ligand Effects and Ligand Design in Homogeneous Gold(I) Catalysis

Weibo Wang, Gerald B. Hammond, and Bo Xu\*

Department of Chemistry, University of Louisville, Louisville, Kentucky 40292, United States

**S** Supporting Information

**ABSTRACT:** Gold catalysis is considered one of the most important breakthroughs in organic synthesis during the past decade, but a rational understanding of ligand effects in gold catalysis is lacking. Most gold-catalyzed reactions go through three major stages: (i) electronic activation of alkyne (or allene) to generate a vinyl gold intermediate; (ii) protodeauration to generate the product and regenerate the cationic gold catalyst; (iii) decay of the active gold catalyst. Our research provides a clearer understanding of how ligands influence each of the three stages in the gold catalytic cycle. What is even more important, by not focusing on a particular gold-catalyzed reaction, we have been able to categorize most gold-catalyzed reactions and propose a ligand design protocol for each category of gold-catalyzed reactions.



## 1. INTRODUCTION

There has been an exponential increase in the number of studies on homogeneous gold catalysis in the past decade.<sup>1–9</sup> Cationic gold species are regarded as the most powerful catalysts for the electrophilic activation of alkynes toward a variety of nucleophiles.<sup>1–8,10,11</sup> The reason for this success is probably due to the lower LUMO properties and poor back-donation of cationic gold species.<sup>12–15</sup> However, the low turnover numbers observed in gold-catalyzed reactions have hindered a wider adoption of gold catalysts in fields such as medicinal chemistry and material synthesis. Considering the fact that gold is a precious metal, the common practice of using 5% loading in gold catalysis makes its use often impractical in larger scale synthesis. Conversely, in many palladium-catalyzed coupling reactions (e.g., Suzuki reaction), the loading can be reduced to parts per million levels.<sup>16</sup>

Ligands play a major role in the tuning of reactivity in transition metal catalysis. Notable examples are Buchwald's palladium-catalyzed reactions such as amination,<sup>17</sup> fluorination,<sup>18</sup> and trifluoromethylation<sup>19</sup> of aryl halides or triflates using custom-made dialkylbiphenyl phosphine ligands. Although a wealth of empirical information on ligand effects is now available on homogeneous gold catalysis,<sup>4</sup> the development of new catalysts and reactions continues to rely upon trial and error, and the outcome of the reaction is often unpredictable. Rational design of suitable ligands to achieve better efficiency is almost nonexistent in gold catalysis.

It is well-accepted that most gold-catalyzed reactions go through three major stages (Scheme 1).<sup>20</sup> In stage 1, a nucleophilic attack on a [AuLn]<sup>+</sup>-activated alkyne (or alkene) proceeds via a  $\pi$ -complex to give a trans-alkenyl gold complex intermediate (or an alkyl gold complex in the case of alkenes). In stage 2, the resulting vinyl complex reacts with an

electrophile (E<sup>+</sup>)—usually a proton—to yield the final product via protodeauration; this step also serves to regenerate the cationic gold species (Scheme 1). In almost all gold-catalyzed reactions, there is a decay or deactivation of the gold catalyst—usually through the reduction of cationic gold to gold(0) (stage 3).

Although the above gold catalytic cycle (Scheme 1) is well-known, it has not provided, for the most part, a rational ligand design to improve efficiency. First of all, there are no conclusive experimental data on how the structure of a ligand affects the kinetics of each stage in the catalytic cycle. For example, it is often assumed that protodemetalation (stage 2) is a relatively fast step in transition metal catalysis; therefore, the electrophilic activation (stage 1) ought to be an important factor in the turnover of a gold catalyst, but this is the case only in a few reactions.<sup>21,22</sup> A case in point is Toste and co-workers' report on the gold-catalyzed hydroamination of allenes<sup>21</sup> and ring expansion of propargyl cyclopropanols.<sup>22</sup> In these two reactions, electron-deficient phosphine ligands (e.g., (*p*-CF<sub>3</sub>C<sub>6</sub>H<sub>4</sub>)<sub>3</sub>P) accelerate the reaction whereas electron-rich phosphine ligands slow down the reaction. However, in a majority of gold-catalyzed reactions, electron-deficient phosphine ligands like (*p*-CF<sub>3</sub>C<sub>6</sub>H<sub>4</sub>)<sub>3</sub>P fare poorly,<sup>4</sup> whereas electron-rich ligands perform better.<sup>23–25</sup> These inconsistencies underlie the complexity of gold catalysis. Moreover, the deactivation of gold is ubiquitous in gold catalysis, and the manner by which a ligand affects gold deactivation is unknown. The deactivation of gold further complicates the predictability of ligand performance in gold catalysis.

Received: February 3, 2012

Published: February 29, 2012

Scheme 1. Typical Gold Catalytic Cycles

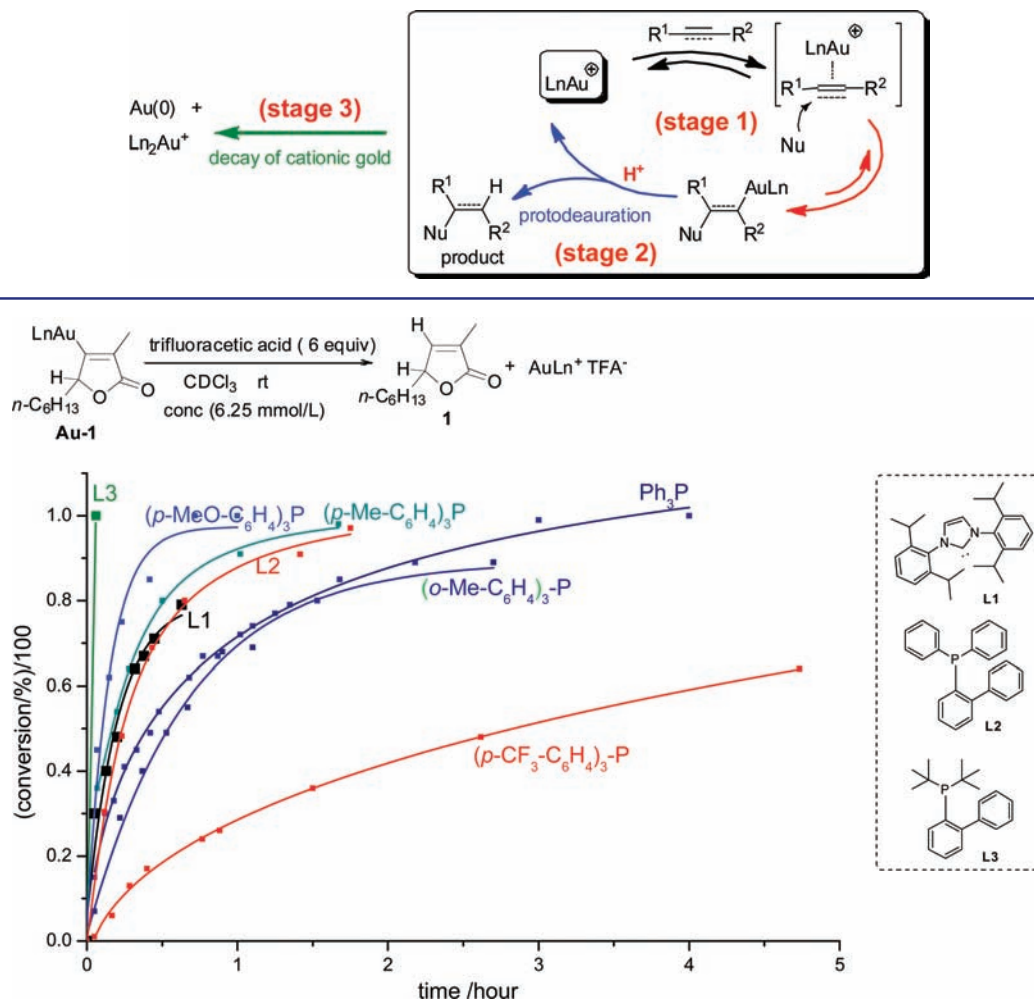


Figure 1. Ligand effects on protodeauration.

We posit that the single reaction analysis will not give us a full understanding of gold-catalyzed reactions. In order to get an overall picture of gold catalysis, we conducted a rational investigation of gold catalysis using the following two-phase strategy:

**1.1. Phase 1.** Establish, experimentally, the structure–activity relationship between a ligand structure and the kinetics of each stage in the gold catalytic cycle. Practitioners in the field assume that electron-deficient ligands promote electrophilic activation (stage 1) and electron-donating ligands promote protodeauration (stage 2). But because the interaction between the ligand and the metal center can be complex (i.e., a ligand can be  $\sigma$ -donor and  $\pi$ -acceptor at the same time), we cannot take the above assumption for granted because it is not backed by conclusive experimental data. The relationship between gold catalyst deactivation and ligand structure is even more elusive, both experimentally and theoretically.

**1.2. Phase 2.** Categorize gold-catalyzed reactions. In theory, there may be two scenarios: the first occurs when protodeauration (stage 2) is the rate-determining step; the second occurs when the electronic activation of alkyne/allene/alkene (stage 1) is the rate-determining step. Because the deactivation of cationic gold (stage 3) is ubiquitous in gold catalysis, we have to consider two additional scenarios: in one case, protodeauration is the rate-determining step and is

accompanied by significant catalyst deactivation; in the second case, electronic activation of alkyne/allene/alkene is the rate-determining step and is accompanied by significant catalyst deactivation. So, in total there may be four categories of gold-catalyzed reactions. Based on the information we obtain in phase 1, we will be able to design suitable ligands for each category.

This two-phase strategy will allow us to understand ligand effects in a rational way, offering a handle on the design of suitable ligands for other reactions we wish to study.

## 2. RESULTS AND DISCUSSION

**2.1.1. Ligand Effects on Each Stage of the Gold Catalytic Cycle (Phase 1).** *Ligand Effects on the Protodeauration Step (Stage 2).* We began our investigation by concentrating on the protodeauration step (stage 2, Scheme 1) because this step not only yields the final product but it also regenerates the cationic gold species that resumes the catalytic cycle. Protodeauration is usually considered a fast process, and therefore it is unlikely to be the rate-determining step in gold catalysis. Very recently, protodeauration of a benzyl gold complex by an alkyne has been investigated by Hashmi and co-workers.<sup>26</sup> Additionally, Blum and co-workers have investigated the relative kinetic basicities of various organogold compounds.<sup>27</sup> But in both cases, no systematic experimental study

on ligand effects on the protodeauration of vinyl gold complexes has been carried out.<sup>28</sup> Since our publication on the isolation and identification of the first ever reported organogold intermediate formed in the gold-catalyzed cyclization of allenates,<sup>29</sup> many other organogold species have been observed.<sup>20,30–35</sup> Because a sleuth of vinyl gold complexes (e.g., **Au-1**, Figure 1) can be prepared readily using our reported method<sup>29</sup> and the reaction with acid gives a clean protodeauration product, we used the protodeauration of complex **Au-1** as our model reaction. First, we investigated the protodeauration of **Au-1** under various acid strengths (see Supporting Information, Table S-1). Weaker acids like acetic acid and chloroacetic acid did not promote the protodeauration of **Au-1**, and protodeauration with a strong acid like TfOH was too fast at room temperature (<10 min) to permit an accurate measurement using in situ NMR. Thus, we used an acid with moderate strength (trifluoroacetic acid, TFA) in our model reaction (Figure 1) and monitored the progress of the reaction through in situ <sup>1</sup>H NMR and <sup>31</sup>P NMR spectroscopy. In <sup>31</sup>P NMR, we clearly observed the disappearance of the vinyl gold complex signal (ca.  $\delta$  44 ppm for **Au-1**, Ln = Ph<sub>3</sub>P) and the regeneration of the cationic gold complex signal (Ph<sub>3</sub>PAu<sup>+</sup>TFA<sup>-</sup>,  $\delta$  29 ppm).

We proceeded to examine the kinetics for the protodeauration for **Au-1** using various ligands. We found that the electronic properties of the ligand have a major influence on the kinetics of the protodeauration: electron-withdrawing groups slowly decrease the rate of the reaction whereas electron-donating groups like OMe increased the reaction rate substantially (Figure 1). We found in all cases that the reaction followed first-order kinetics (large excess of acid was used; hence, the concentration of the acid was considered constant). The plot of  $\ln(A/A_0)$  vs time showed good linear correlation (Figure 2), allowing the calculation of the  $k_{\text{obs}}$  of protodeaura-

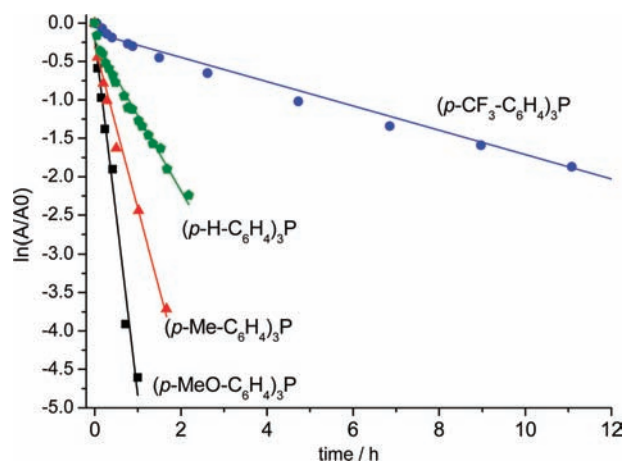


Figure 2. Protodeauration of **Au-1** showing first-order kinetics.

tion of **Au-1** gold complex with various para-substituted Ar<sub>3</sub>P-type ligands. We conducted a Hammett correlation study to determine the quantitative electronic influence of ligands and found good correlation for the protodeauration process ( $\rho = -4.03$ ,  $R^2 = 0.98$ ) (Figure 3). The negative  $\rho$  value ( $<-1$ ) indicates that it is sensitive to the influence of substituents and that positive charge is built on the reaction center. In addition to screening Ar<sub>3</sub>P-type ligands, we examined other commonly used ligands such as NHC carbene-type ligands IPr (**L1**). A NHC carbene ligand is generally considered electron-rich

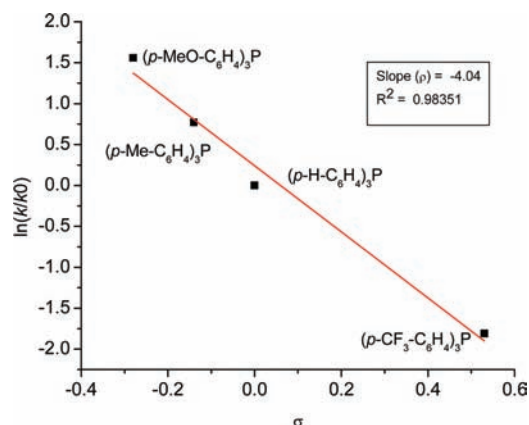
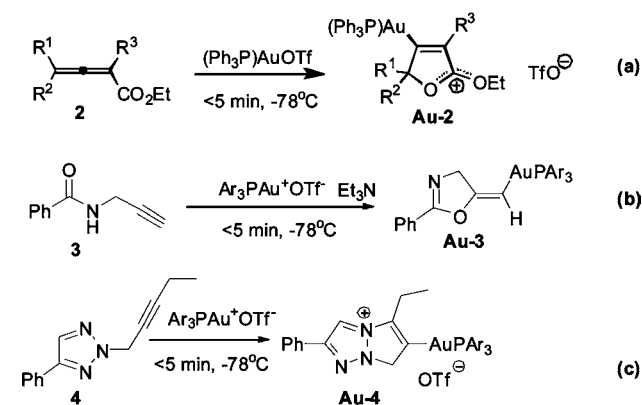


Figure 3. Hammett correlation on protodeauration of **Au-1**.

compared to a standard Ph<sub>3</sub>P ligand, and protodeauration of its corresponding vinyl gold complex is indeed faster (Figure 1). Steric effects seem to influence the kinetics of the protodeauration step: the sterically more demanding (*o*-Me-C<sub>6</sub>H<sub>4</sub>)<sub>3</sub>P slowed the reaction compared with (*p*-Me-C<sub>6</sub>H<sub>4</sub>)<sub>3</sub>P, but the ligand (*o*-Ph-C<sub>6</sub>H<sub>4</sub>)Ph<sub>2</sub>P (**L2**) promoted protodeauration; this fact may be attributed to the possibility that an ortho-substituted phenyl ring stabilizes the generated cationic gold complex through a  $\eta^2$ -interaction.<sup>36</sup> In our hands, Buchwald biaryl phosphine-type ligand **L3** gave the fastest protodeauration rate; this result could be rationalized by the presence of biphenyl and two electron-rich alkyl substitutions on the phosphine center. We also investigated the effect of acid concentration on the protodeauration step. In general, a higher concentration of acid gives a higher rate of protodeauration. Of course, factors other than ligand species could also affect the protodeauration. For example, a very recent report by Gagné and co-workers indicates that in the presence of excess amount of cationic gold, geminal digold formation may affect the kinetics of protodeauration.<sup>37</sup> Our research, though, delineates how the electronic properties of a ligand affect the kinetics of protodeauration and provides guidelines in the design of novel ligands for gold catalysis.

**2.1.2. Ligand Effects on Electronic Activation of Alkyne/Allene (Stage 1).** As mentioned earlier, we were the first to isolate and identify the organogold intermediate formed in the gold-catalyzed cyclization of allenates (Scheme 2a).<sup>29</sup> Many other organogold species have been reported since (Scheme 2).<sup>20,30–34,38</sup> For example, Hashmi and co-workers have

#### Scheme 2. Formation of Gold Complexes

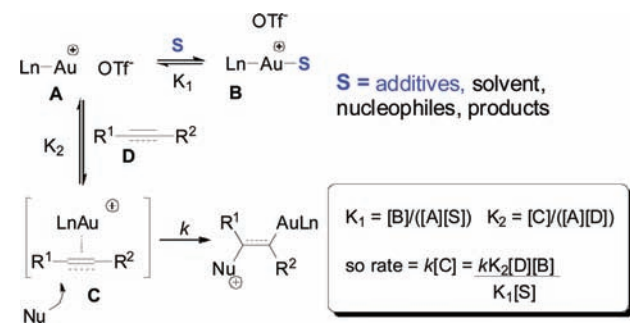




identified an Au-3-type structure in the gold-catalyzed cyclization of propargyl amide<sup>30,39</sup> whereas Shi and co-workers have identified a Au-4-type<sup>31</sup> structure. Toste and co-workers have studied ligand effects on the intramolecular aminoauration of alkenes, but the electronic influence of the ligand on the kinetics of this process appears to follow a complex pattern.<sup>34</sup> Because the gold-catalyzed reaction of alkynes is much faster than the corresponding alkenes, we investigated ligand effects on the kinetics of this fundamental step using in situ NMR and IR spectroscopy. We started by conducting a preliminary study on the kinetics of our three model systems (Scheme 2) but found that in all these systems the reaction was complete almost instantly at room temperature, which hindered our kinetic measurements (see Supporting Information, Figure S-1). We resorted to low-temperature in situ NMR and IR spectroscopy, but these reactions were still too fast (<5 min) even at -78 °C (Scheme 2), signaling the fact that the electronic activation step for the intramolecular reactions of 2, 3, and 4 may not be the rate-determining step.

We then switched our attention to model reaction C (Scheme 2c), because the isolable gold vinyl complex Au-4 has excellent stability toward protodeauration.<sup>31</sup> Au-4 can transform itself into Au-5 over time, but it is a much slower process compared to the formation of Au-4. Reaction C is an ideal model because there are no concerns that a possible protodeauration will influence the kinetics of vinyl gold formation. In gold-catalyzed reactions, cationic gold usually will coordinate with additives, solvent, nucleophiles, or even products (Scheme 3). In order to slow down the reaction,

### Scheme 3. Formation of Gold Complex in the Presence of S-Competition



facilitate the kinetic study, and mimic the competition of the nucleophile with cationic gold species, we added different additives to the reaction mixture such as sulfide and benzotriazole; both additives slowed down the reaction significantly (see Supporting Information, Figure S-2), but because benzotriazole has a similar functional group as the starting material we carried our model reaction C in the presence of excess amounts of benzotriazole.

The results are shown in Figure 4. In general, electron-rich ligands such as dialkylbiphenyl phosphine slowed the reaction (Figure 4), whereas a gold complex with an electron-poor ligand (e.g., (*p*-CF<sub>3</sub>C<sub>6</sub>H<sub>4</sub>)<sub>3</sub>P) accelerated the conversion to vinyl gold complex Au-4. Most other Ar<sub>3</sub>P-type ligands possessing moderate electron density yield very similar initial reaction rates (Figure 4). It should be noted that in all cases, even when the starting material 4 was present in large excess (3 equiv), the reaction did not go to completion (Figure 4). This phenomenon highlights the highly reversible nature of this

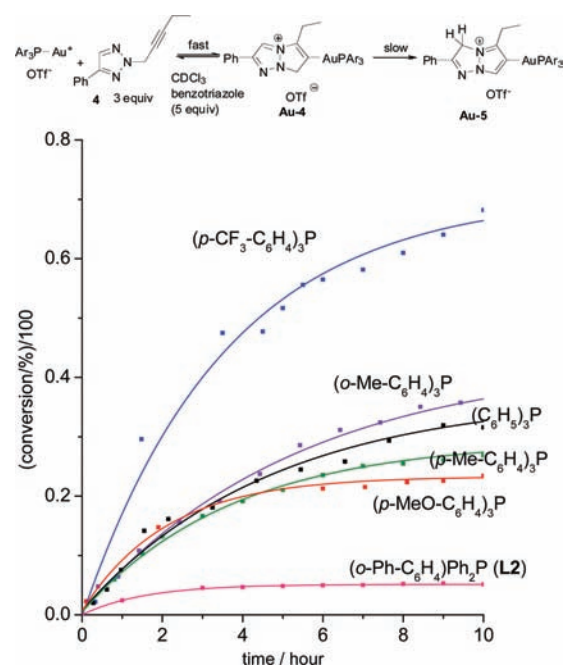


Figure 4. Ligand effects in the formation of gold complex Au-4.

transformation. It has been shown by Toste<sup>34</sup> and others<sup>40</sup> that a nucleophilic attack on the coordinated alkene can be reversible. In general, electron-poor ligands give better conversion than electron-rich ligands (Figure 4). Of course, electron-poor ligands could yield a higher conversion due to thermodynamic effects rather than kinetic effects. But analysis of the initial reaction rate (when time = 0, Figure 4) indicates that the initial reaction rate is faster for electron-poor ligands. So, it appears most likely that this process is favored by electron-poor ligands, both thermodynamically and kinetically.

The data shown in Figure 4 also reveal the complex nature of this process. For example, Ar<sub>3</sub>P-type ligands with moderate electron density yield very similar initial reaction rates. The rationalization of this trend is depicted in Scheme 3. Unlike the protodeauration case, the nucleophilic attack on the gold-activated alkyne/allene/alkene may not be a simple elementary step: the cationic gold species could coordinate with an alkyne/allene/alkene substrate to generate a  $\eta^2$ -complex before the nucleophile attack takes place. But in order to form the  $\eta^2$ -complex C, the alkyne substrate has to compete with additives, solvent, nucleophiles, or even products that can also coordinate with the cationic gold species. Also, the formation of C may not even be thermodynamically favorable ( $K_1 \gg K_2$ ). Stradiotto and co-workers have reported that amine nucleophiles have much higher affinity toward cationic gold than alkynes.<sup>41</sup> The complexation of cationic gold with alkynes/alkenes is supposed to be fast, and equilibrium should be reached (Scheme 3). The overall rate of gold complex formation will then be  $kK_2[\text{D}][\text{B}]/K_1[\text{S}]$  (Scheme 3). While the rate constant  $k$  may directly correlate with the electron density of phosphine ligands, it is no longer the only factor that determines the overall rate, which will be also controlled by  $K_2/K_1$  (Scheme 3). This may explain why most other Ar<sub>3</sub>P-type ligands with moderate electron density have very similar initial reaction rates. Because in our model reaction benzotriazole competes with the alkyne substrate in the coordination with cationic gold ( $K_1 \gg K_2$ ), this reaction is significantly slowed down in the presence of benzotriazole.

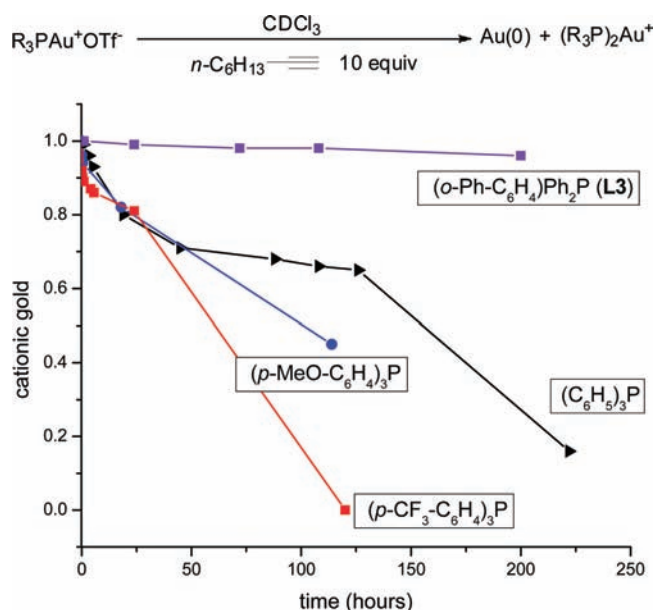


Figure 5. Ligand effects on the decay of cationic gold ( $R_3PAu^+OTf^-$ ).

**2.1.3. Ligand Effects on the Decay of Cationic Gold (Stage 3).** In most gold catalytic reactions, turnover is low because, among other factors, cationic gold is gradually reduced to gold(0) (precipitated gold particles or sometimes a gold mirror appear in gold-catalyzed reactions) and  $Ln_2Au^+$  forms.  $Ln_2Au^+$  is no longer an active cationic species because gold(I) has a linear bicoordinated geometry. Despite its importance, the gold decay step has never been studied systematically. We found that standard cationic gold  $Ph_3PAu^+OTf^-$  in solution is rather stable (no significant decomposition occurred after several days standing at room temperature and monitored by  $^{31}P$  NMR), but when a reductive substrate (e.g., alkyne) was added to the solution, the gold complex decayed at a fast rate. The decay of

various cationic gold species is shown in Figure 5. All para-substituted  $Ar_3PAu^+$  complexes exhibit significant decay over time at room temperature. The electronic effects of the ligands seem not to have a major influence on the stability of cationic gold: both electron-richer and electron-poorer ligands (compared to  $Ph_3P$ ) lead to faster decay. Gold(I) complexes with a Buchwald-type biphenyl phosphine ligand were introduced as gold ligands by Echavarren and co-workers in 2005.<sup>42</sup> These workers found that a weak interaction may exist between the Au center and the arene moiety parallel to the PAu bond.<sup>36</sup> Zhang and co-workers also reported that a  $\eta^2$ -interaction may exist in a phosphinamidite-gold(I) complex fitted with an anthracene moiety,<sup>43</sup> but no experimental study comparing the relative stability of cationic gold with different ligands has been conducted to date. We tested a biphenyl diaryl phosphine ligand and found that, indeed, it is very stable under the same conditions (Figure 5). We propose that a  $\eta^2$ -interaction may account for the higher stability of biphenyl gold(I) complexes, but a more recent study by Echavarren and co-workers indicated that this interaction can be very weak because the gold-arene distance is longer than the maximum estimated for a meaningful metal-arene interaction. A clearer understanding of the underlying mechanism for this stabilization will need to wait for more detailed investigations. Although the decay is highly dependent on the nature of the reaction it catalyzes, our research sheds some light on how the structure of ligand could affect the rate of decay of the gold species.

## 2.2. Categorizing Gold-Catalyzed Reactions (Phase 2).

The above kinetic studies on individual stages in the gold catalytic cycles yielded valuable information on how to design ligands with high turnover numbers in a given reaction. We do not expect that one single ligand will work for all gold-catalyzed reactions because different reactions have different rate-determining steps, but we believe that a certain amount of predictability can be achieved if gold-catalyzed reactions are categorized as follows.

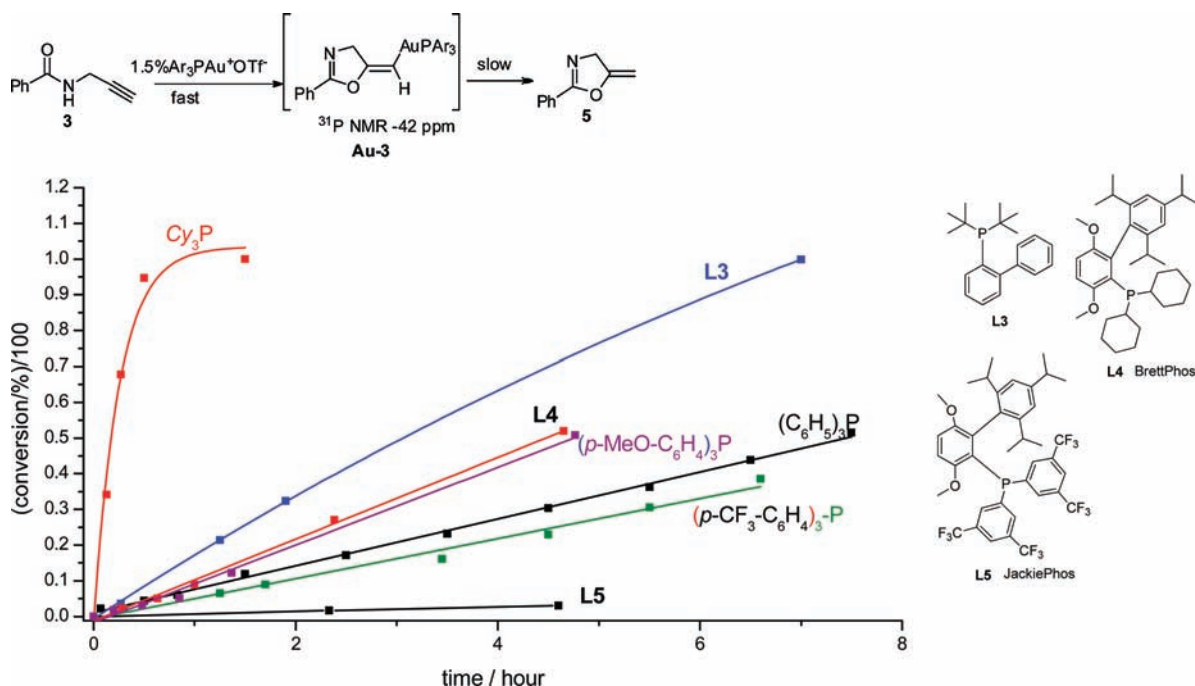


Figure 6. Ligand effects on the gold-catalyzed cyclization of propargyl amide 3.

**2.2.1. Protodeauration Is the Rate-Determining Step.** The gold-catalyzed cyclization of propargyl amide, which offers a mild access to oxazole derivatives, has found many application in synthesis.<sup>44</sup> Hashmi and co-workers have identified the vinyl gold intermediate in this reaction (derivative of Au-3).<sup>30</sup> The standard gold cationic species,  $\text{Ph}_3\text{PAu}^+$ , used for this transformation showed a low turnover frequency (TOF) (1–5% Au loading, 24–48 h at rt) and a low turnover number.<sup>44</sup> During our kinetic studies on the formation of vinyl gold complexes (Scheme 2), we found that the formation of vinyl gold complex Au-3 is indeed a very fast process; the reaction is over before NMR detection can be carried out (less than 5 min), even at  $-78^\circ\text{C}$  (Scheme 2). This observation led us to believe that the gold complex formation step is not the rate-determining step.  $^{31}\text{P}$  NMR monitoring of this reaction also indicated that the resting state for the gold catalyst in this transformation is a vinyl gold complex. Therefore, it is reasonable to assume that the protodeauration step is slow and therefore is the rate-determining step.

According to our above studies on ligand effects on the kinetics of the protodeauration process (Figure 1), an electron-rich ligand will accelerate this process; therefore, a gold catalyst with an electron-rich ligand ought to deliver a higher turnover frequency compared to a standard  $\text{Ph}_3\text{PAu}^+$ . Our experiments support this statement. Ligand effects on the kinetics of the cyclization of propargyl amide 3 are shown in Figure 6. Electron-poor ligands slow the reaction rate compared to electron-rich ligands. The ligand effect in the cyclization of 3 is similar to the protodeauration process (Figure 2). Thus, it is not surprising to find that the highly electron-rich trialkyl phosphine ligand gives the fastest conversion (Figure 6). We also tested two other Buchwald-type diphenyl phosphine ligands; again, the electron-richer ligand L4 (BrettPhos) delivers a fast transformation compared to the relatively electron-poor ligand L5 (JackiePhos) (Figure 6).

We found that this reaction followed zero-order kinetics (linear relationship between conversion and time), which means that the rate of the reaction is independent of the concentration of starting material 4. This result shores up support for the assumption that protodeauration is the rate-determining step: the protodeauration of Au-3 does not involve starting material 3, so the overall reaction rate is independent of the concentration of 3.

As in our above study of the protodeauration process, we conducted a Hammett correlation investigation to determine the quantitative electronic influence of ligands and found a good correlation for the cyclization of propargyl amide 3 (Figure 8). The Hammett correlation also showed good linear correlation ( $\rho = -0.89$ ). The negative value  $\rho$  confirms the fact that the reaction is accelerated by electron-donating groups on the ligand. The rate for the overall reaction is proportional to the concentration of gold catalyst (Figure 7). This finding is also consistent with our conclusion that protodeauration is the rate-determining step. It should be noted that the rate of the reaction is kept constant until the gold catalyst becomes the limiting reagent; this factor indicates that the deactivation of gold is minimal during course of this reaction.

**2.2.2. Electronic Activation of Alkyne (Or Allene/Alkene) Is the Rate-Determining Step.** We expect the electronic activation of alkyne (or allene/alkene) to be the rate-determining step when the nucleophile is relatively weak or when the substrate is a less reactive alkene or allene. In these situations, a strong electronic activation from cationic gold is

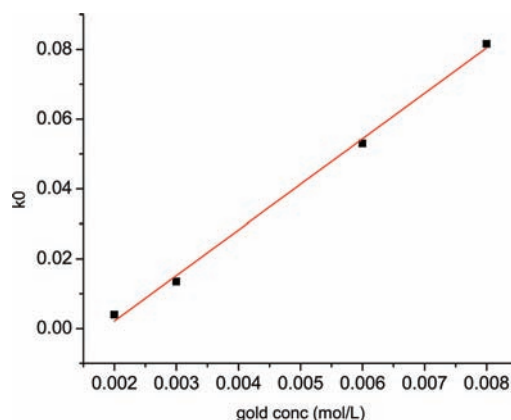


Figure 7. Reaction rate vs gold concentration.

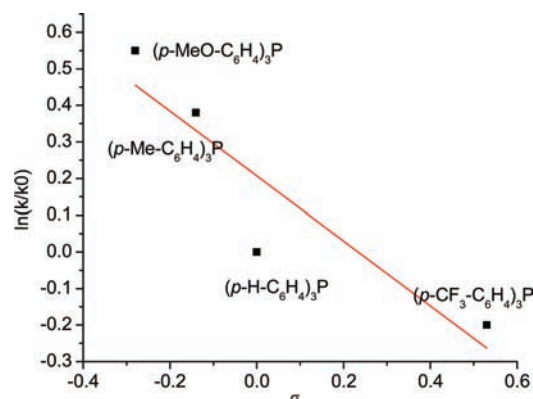
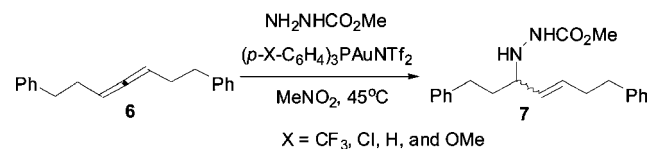


Figure 8. Hammett equation for the cyclization of propargyl amide 3.

needed. We have demonstrated that an electron-poor ligand will facilitate the vinyl gold complex formation step (Figure 4); therefore, an electron-poor ligand should accelerate the overall reaction rate in reactions of this type. One elegant study that supports this statement is the intermolecular hydroamination of allenes with hydrazide in the presence of  $\text{LnAuNTf}_2$  (Scheme 4), first reported by Toste and co-workers.<sup>21</sup> Because allenes

#### Scheme 4. Electronic Activation Is the Rate-Determining Step



are less reactive than alkynes toward nucleophilic attack and the electron-deficient hydrazide is a relatively weak nucleophile, the electronic activation of the allene becomes the rate-determining step. Toste and co-workers found that the reaction followed pseudo-first-order kinetics in allene 6 (Scheme 4).<sup>21</sup> The first-order dependence implies that the allene starting material 6 is involved in the rate-determining step. The authors also conducted a Hammett study of the reaction to probe its sensitivity to changes in the electronic properties of the phosphine ligand in  $(p\text{-X-C}_6\text{H}_4)_3\text{PAuNTf}_2$  (X = CF<sub>3</sub>, Cl, H, and OMe). The kinetic order and positive  $\rho$  value (+0.21) in the Hammett analysis of the reaction are consistent with gold(I) activation of allene being the rate-limiting step in the catalytic cycle.



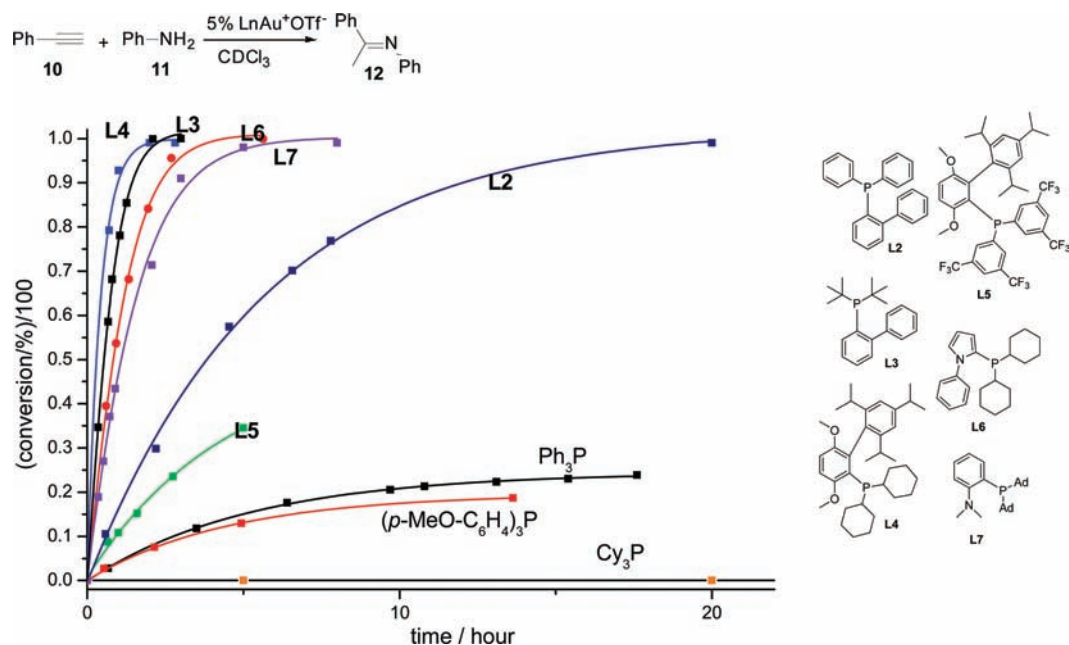


Figure 9. Ligand effects on an intermolecular hydroamination reaction.

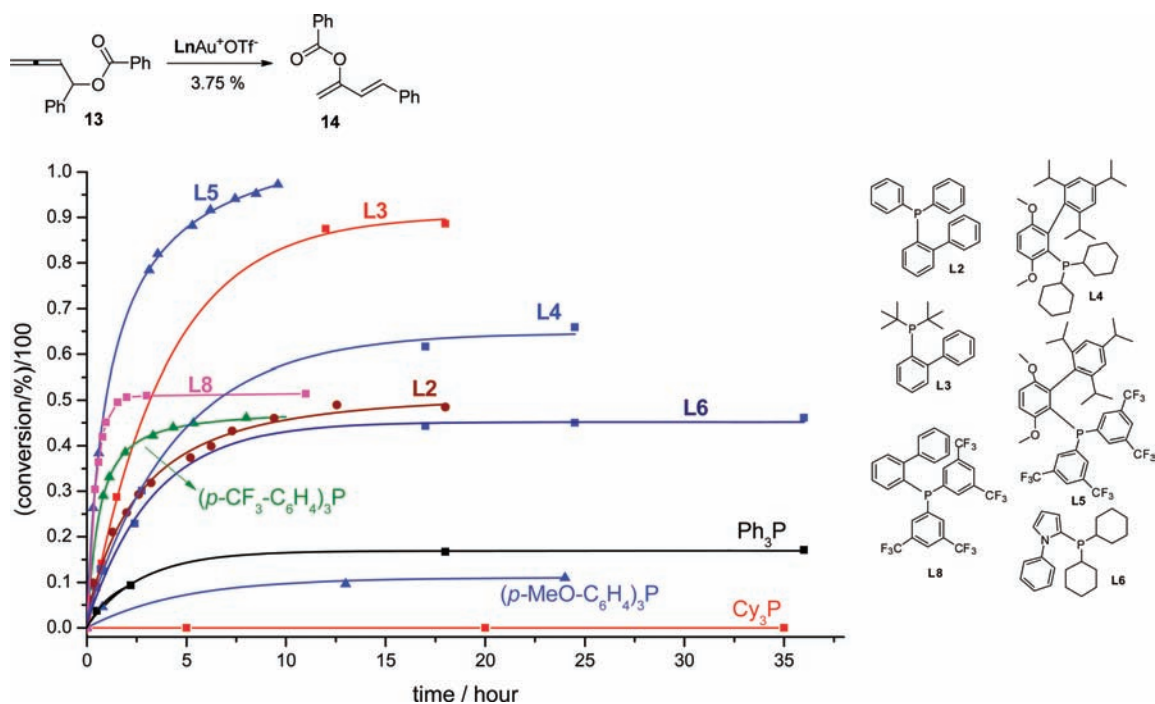


Figure 10. Ligand effect in the rearrangement of allenyl ester.

**2.2.3. Protodeauration Is the Rate-Determining Step and Catalyst Deactivation Is Significant.** In the two model reactions discussed above, the deactivation of an active gold catalyst was not regarded as significant. But this is not the case for many gold-catalyzed reactions. A case in point is the transition-metal-catalyzed hydroamination, namely, the direct formation of a new C–N bond by addition of an amine to an unsaturated carbon–carbon bond via an atom-efficient pathway.<sup>45</sup> In the gold-catalyzed addition of basic nitrogen nucleophiles (e.g., aliphatic/aromatic amine) to alkynes/allenes/alkenes, any acid in the reaction system is neutralized or weakened by the presence of large amounts of a basic

substance (amine) in the reaction mixture. According to our study on protodeauration (see Supporting Information, Table S-1), the protodeauration step will be slower, or may not even proceed, in the presence of weak acids. So, it is very likely that protodeauration is the rate-determining step in this type of reaction. The model reaction we constructed for this scenario is the intermolecular amination of phenyl acetylene (shown in Figure 9). A simple kinetic profiling for this reaction, using 5% standard  $\text{Ph}_3\text{PAu}^+\text{OTf}^-$ , showed that the rate of the reaction decreased significantly during the course of the reaction. The reaction proceeded at a reasonable rate during its initial stage, but the rate decreased significantly over time and the maximum

conversion hovered only around 20%. This phenomenon signals a significant catalyst deactivation during the course of the reaction.

Additional results on ligand effects on the intermolecular hydroamination reaction are presented in Figure 9. Because protodeauration may be the rate-determining step, we decided to use an electron richer ligand (*p*-MeO-C<sub>6</sub>H<sub>4</sub>)<sub>3</sub>P (compared to Ph<sub>3</sub>P). It gave a faster initial reaction rate, but its longer-term performance was even worse than with Ph<sub>3</sub>P, perhaps due to its faster decay (Figure 5). The Cy<sub>3</sub>P ligand, which is regarded as the best ligand for the cyclization of propargyl amides, did not catalyze the hydroamination reaction due to its facile deactivation. According to our cationic gold decay experiments (Figure 5), *σ*-phenyl substitution on the R<sub>3</sub>P ligand may slow down the decay of cationic gold. Therefore, we switched from Ph<sub>3</sub>P to (*o*-Ph-C<sub>6</sub>H<sub>4</sub>)Ph<sub>2</sub>P (L2). This ligand was superior to Ph<sub>3</sub>P as demonstrated by the fact that the reaction was 100% complete after 20 h at room temperature. This result also indicates that the deactivation of the cationic gold catalyst had been significantly slowed down. Based on our findings on the protodeauration step (Figure 2), an electron-rich ligand should speed up this step; therefore, an electron-rich ligand is needed for a high TOF in this type of reaction. If we combine these two effects, then an electron-rich ligand with *σ*-phenyl substitution should be optimal. Indeed, we found this to be the case: an electron-rich ligand with  $\eta^2$ -stabilization such as L4 gave the best results in our hydroamination reaction (Figure 6). Thus, the rate of the overall reaction is dependent on the concentration of gold catalyst and is proportional to its concentration (see Supporting Information, Figure S-3). This observation is also consistent with our conclusion that protodeauration is the rate-determining step.

**2.2.4. Electronic Activation of Alkyne/Allene/Alkene Is the Rate-Determining Step and Is Accompanied by Significant Catalyst Deactivation.** As we discussed earlier, the electronic activation of an unsaturated C–C bond may be the rate-determining step in cases when the nucleophile is relatively weak or the substrate is a less reactive alkene or allene. We chose the gold(I)-catalyzed isomerization of allenyl carbinol ester as a model for this type of reaction because the substrate is an allene and the nucleophile is a weak carbonyl oxygen. This reaction has been reported as an efficient way to access functionalized 1,3-butadiene-2-ol esters.<sup>46</sup> Our results on ligand effects are illustrated in Figure 10. When Ph<sub>3</sub>PAuOTf was used, the reaction proceeded at a reasonable rate in its initial stage, but the rate decreased over time significantly and the maximum conversion reached only 15%. This behavior shows that a significant decay of the active gold complex had occurred. Because the rate-determining step for this reaction may be the electronic activation of the allene, we surmised that an electron-poor ligand ought to speed up this step (see Figure 2). Therefore, an electron-poor ligand is needed if one is to obtain a high TOF in this type of reaction. Accordingly, we chose an electron-poorer ligand (*p*-CF<sub>3</sub>-C<sub>6</sub>H<sub>4</sub>)<sub>3</sub>P (compared to Ph<sub>3</sub>P); this ligand promoted a faster initial reaction rate but still showed signs of catalyst decay. According to our cationic gold decay experiments (Figure 5), *σ*-phenyl substitution on Ar<sub>3</sub>P may slow down the decay of cationic gold. Therefore, we switched to (*o*-Ph-C<sub>6</sub>H<sub>4</sub>)Ph<sub>2</sub>P (L2); this ligand was vastly superior to Ph<sub>3</sub>P, as the maximum conversion increased from 15% to 50% at room temperature. The deactivation of cationic gold catalyst seemed to have been significantly reduced. We proceeded to combine the two effects, namely, the use of an

electron-poor ligand with *o*-phenyl substitution. First, we evaluated a biphenyl diphenyl ligand substituted with an electron-withdrawing group (L8); it worked even better than (*o*-Ph-C<sub>6</sub>H<sub>4</sub>)Ph<sub>2</sub>P (L2) but could not prevent the deactivation of gold over time. We hypothesized that an additional substitution on the *o*-phenyl ring may help to further increase the stability of cationic gold and were rewarded when we found that the electron-poor L5 produced the best results in this rearrangement reaction (Figure 10). This ligand showed high reactivity during the entire course of the reaction. Electron-rich biphenyl phosphine ligands L3, L4, and L6 gave less satisfying results. Again the Cy<sub>3</sub>P ligand, which was the best ligand in the cyclization of propargyl amide, did not catalyze this reaction, possibly because of its electron-rich nature and fast deactivation.

### 3. SUMMARY

Although for each one of our four categories of gold-catalyzed reactions we have only chosen one example for discussion, we believe most gold-catalyzed reactions will fit our four categories. Of course, many gold-catalyzed reactions may incur extra steps (e.g., rearrangement) during the catalytic cycle, or the starting material or product may follow alternative pathways to give other byproducts. We propose that each category has an optimized set of catalysts, summarized in Scheme S-1 in the Supporting Information section. We have surveyed representative gold-catalyzed reactions, but detailed kinetic information on each reaction can be found in the Supporting Information section. The impact of our studies may not be limited to gold catalysis but may also serve to offer general guidance to improve understanding of transition metal catalysis in general.

### ■ ASSOCIATED CONTENT

#### 📄 Supporting Information

General experimental procedures and additional kinetic data. This material is available free of charge via the Internet at <http://pubs.acs.org>.

### ■ AUTHOR INFORMATION

#### Corresponding Author

Bo.xu@louisville.edu

#### Notes

The authors declare no competing financial interest.

### ■ ACKNOWLEDGMENTS

We are grateful to the National Science Foundation for financial support (CHE-1111316) and acknowledge the support provided by the CREAM Mass Spectrometry Facility (University of Louisville) funded by NSF/EPSCoR (EPS-0447479).

### ■ REFERENCES

- (1) Hashmi, A. S. K. *Chem. Rev.* **2007**, *107*, 3180.
- (2) Garcia, P.; Malacria, M.; Aubert, C.; Gandon, V.; Fensterbank, L. *ChemCatChem* **2010**, *2*, 493.
- (3) Arcadi, A. *Chem. Rev.* **2008**, *108*, 3266.
- (4) Gorin, D. J.; Sherry, B. D.; Toste, F. D. *Chem. Rev.* **2008**, *108*, 3351.
- (5) Jimenez-Nunez, E.; Echavarren, A. M. *Chem. Rev.* **2008**, *108*, 3326.
- (6) Li, Z.; Brouwer, C.; He, C. *Chem. Rev.* **2008**, *108*, 3239.
- (7) Hashmi, A. S. K.; Rudolph, M. *Chem. Soc. Rev.* **2008**, *37*, 1766.
- (8) Widenhofer, R. A. *Chem.—Eur. J.* **2008**, *14*, 5382.



- (9) Rudolph, M.; Hashmi, A. S. K. *Chem. Soc. Rev.* **2012**, *41*, 2448.
- (10) Benitez, D.; Shapiro, N. D.; Tkatchouk, E.; Wang, Y.; Goddard, W. A.; Toste, F. D. *Nat. Chem.* **2009**, *1*, 482.
- (11) Teles, J. H.; Brode, S.; Chabanas, M. *Angew. Chem., Int. Ed.* **1998**, *37*, 1415.
- (12) Gorin, D. J.; Toste, F. D. *Nature (London, U.K.)* **2007**, *446*, 395.
- (13) Hertwig, R. H.; Koch, W.; Schröder, D.; Schwarz, H.; Hrušák, J.; Schwerdtfeger, P. *J. Phys. Chem.* **1996**, *100*, 12253.
- (14) Pernpointner, M.; Hashmi, A. S. K. *J. Chem. Theory Comput.* **2009**, *5*, 2717.
- (15) Lein, M.; Rudolph, M.; Hashmi, S. K.; Schwerdtfeger, P. *Organometallics* **2010**, *29*, 2206.
- (16) Shen, Q.; Shekhar, S.; Stambuli, J. P.; Hartwig, J. F. *Angew. Chem., Int. Ed.* **2005**, *44*, 1371.
- (17) Fors, B. P.; Watson, D. A.; Biscoe, M. R.; Buchwald, S. L. *J. Am. Chem. Soc.* **2008**, *130*, 13552.
- (18) Watson, D. A.; Su, M.; Teverovskiy, G.; Zhang, Y.; Garcia-Fortanet, J.; Kinzel, T.; Buchwald, S. L. *Science* **2009**, *325*, 1661.
- (19) Cho, E. J.; Senecal, T. D.; Kinzel, T.; Zhang, Y.; Watson, D. A.; Buchwald, S. L. *Science* **2010**, *328*, 1679.
- (20) Hashmi, A. S. K. *Angew. Chem., Int. Ed.* **2010**, *49*, 5232.
- (21) Wang, Z. J.; Benitez, D.; Tkatchouk, E.; Goddard, W. A. III; Toste, F. D. *J. Am. Chem. Soc.* **2010**, *132*, 13064.
- (22) Markham, J. P.; Staben, S. T.; Toste, F. D. *J. Am. Chem. Soc.* **2005**, *127*, 9708.
- (23) Leyva, A.; Corma, A. *J. Org. Chem.* **2009**, *74*, 2067.
- (24) Zhang, D.-H.; Yao, L.-F.; Wei, Y.; Shi, M. *Angew. Chem., Int. Ed.* **2011**, *50*, 2583.
- (25) Leyva-Pérez, A.; Cabrero-Antonino, J. R.; Cantín, A. n.; Corma, A. *J. Org. Chem.* **2010**, *75*, 7769.
- (26) Hashmi, A. S. K.; Braun, I.; Rudolph, M.; Rominger, F. *Organometallics* **2012**, *31*, 644.
- (27) Roth, K. E.; Blum, S. A. *Organometallics* **2010**, *29*, 1712.
- (28) Krauter, C. M.; Hashmi, A. S. K.; Pernpointner, M. *ChemCatChem* **2010**, *2*, 1226.
- (29) Liu, L.-P.; Xu, B.; Mashuta, M. S.; Hammond, G. B. *J. Am. Chem. Soc.* **2008**, *130*, 17642.
- (30) Hashmi, A. S. K.; Schuster, A. M.; Rominger, F. *Angew. Chem., Int. Ed.* **2009**, *48*, 8247.
- (31) Chen, Y.; Wang, D.; Petersen, J. L.; Akhmedov, N. G.; Shi, X. *Chem. Commun.* **2010**, *46*, 6147.
- (32) Weber, D.; Tarselli, M. A.; Gagné, M. R. *Angew. Chem., Int. Ed.* **2009**, *48*, 5733.
- (33) Zhu, Y.; Yu, B. *Angew. Chem., Int. Ed.* **2011**, *50*, 8329.
- (34) LaLonde, R. L.; Brenzovich, W. E. Jr.; Benitez, D.; Tkatchouk, E.; Kelley, K.; Goddard, W. A. III; Toste, F. D. *Chem. Sci.* **2010**, *1*, 226.
- (35) Döpp, R.; Lothschütz, C.; Wurm, T.; Pernpointner, M.; Keller, S.; Rominger, F.; Hashmi, A. S. K. *Organometallics* **2011**, *30*, 5894.
- (36) Herrero-Gómez, E.; Nieto-Oberhuber, C.; López, S.; Benet-Buchholz, J.; Echavarren, A. M. *Angew. Chem., Int. Ed.* **2006**, *45*, 5455.
- (37) Weber, D.; Jones, T. D.; Adduci, L. L.; Gagné, M. R. *Angew. Chem., Int. Ed.* **2012**, in press, DOI: 10.1002/anie.201107659.
- (38) Melchionna, M.; Nieger, M.; Helaja, J. *Chem.—Eur. J.* **2010**, *16*, 8262.
- (39) Hashmi, A. S. K.; Schuster, A. M.; Gaillard, S.; Cavallo, L.; Poater, A.; Nolan, S. P. *Organometallics* **2011**, *30*, 6328.
- (40) de Haro, T.; Nevado, C. *Angew. Chem., Int. Ed.* **2011**, *50*, 906.
- (41) Hesp, K. D.; Stradiotto, M. *J. Am. Chem. Soc.* **2010**, *132*, 18026.
- (42) Nieto-Oberhuber, C.; López, S.; Echavarren, A. M. *J. Am. Chem. Soc.* **2005**, *127*, 6178.
- (43) Li, Q.-S.; Wan, C.-Q.; Zou, R.-Y.; Xu, F.-B.; Song, H.-B.; Wan, X.-J.; Zhang, Z.-Z. *Inorg. Chem.* **2006**, *45*, 1888.
- (44) Weyrauch, J. P.; Hashmi, A. S. K.; Schuster, A.; Hengst, T.; Schetter, S.; Littmann, A.; Rudolph, M.; Hamzic, M.; Visus, J.; Rominger, F.; Frey, W.; Bats, J. W. *Chem.—Eur. J.* **2010**, *16*, 956.
- (45) Muller, T. E.; Hultsch, K. C.; Yus, M.; Foubelo, F.; Tada, M. *Chem. Rev.* **2008**, *108*, 3795.
- (46) Buzas, A. K.; Istrate, F. M.; Gagosz, F. *Org. Lett.* **2007**, *9*, 985.